Institute of Space and Aeronautical Science, University of Tokyo
Report No. 477, March 1972

A Free-Flight Support System

By

Akira AZUMA, Bunji TOMITA*, Matsusaburo IUCHI,
Hideo MISHIMA**, Tadami IWATA** and Akira KOMOTO**

Summary: This is the second part of the report titled "A New Running Test Facility for the Study of Flight Dynamics" [*1*]. A support system for free flight of a model aircraft simulated to V/STOL plane or helicopter has been constructed as an additional equipment for the running test facility. The support system is consisted of a free-flight follower and a data reduction system. The free-flight follower can be carried on a carriage moving on a track and supports the model as it can fly either freely or in partly constrained freedom. The flight path and attitude angles of the model during flight can be sensed with potentiometers on the support system and recorded in oscillograms or stored in memories of a miniature computer through an A-D converter, a part of or all of which are boarded on the carriage as the data reduction system.

By analyzing the data the aero and/or flight dynamic characteristics of the model will be obtained.

1. INTRODUCTION

As described in the preceding paper [*1*] the running test facility can be used for the study of aero and/or flight dynamics with a flying model supported on a free-flight follower. The follower must be able to follow or pursue the linear motion and allow the rotational motion of the model so as to sustain the model very freely or in restricted condition with respect to the unnecessary directions. To attain the above object the follower may be provided with a servo system having hydraulic driving units and position sensors which can detect the linear and angular motions of the model by potentiometers.

The model can, sometimes, be a simulation model which is dynamically similar to an actual aircraft in aero- and flight-dynamic senses so that the time factor, which is used to normalize the time dimension, must be reduced and the natural frequency must be increased for a small scale model. Therefore the response of the free-flight follower to pursue the model motion must be high enough to keep the model in free flight condition as shown in Table 1 derived from the similarity law (See Appendix).

It will be appreciated that the free-flight follower should be constructed as light as possible to satisfy the above requirements without lacking the stiffness of the follower.

* National Space Development Agency of Japan
** Shimadzu Seisakusho Ltd.

The motion of the model traced by the follower can be sensed as voltage outputs of the potentiometers and be recorded either directly or through an analogu data recorder into a data reduction system. The data reduction system is usually arranged in a computer room but can be borded on the carriage if necessary. The data reduction system can store the sampling data of the linear and angular displacements of the model motion in memories through an A-D converter and process them with a central processing unit according to a specified instruction. The sampling period must be short enough to reproduce the model motion precisely. The analogue data recorder can transfers the data to the data reduction system at any time in case of necessity.

Since the model motion is observed for less than twenty seconds the maximum capacity of the computer memories can be decided so as to get the necessary informations with satisfactory accuracy while the motion is not damped out.

The block diagram of the total system is shown in Fig. 1.

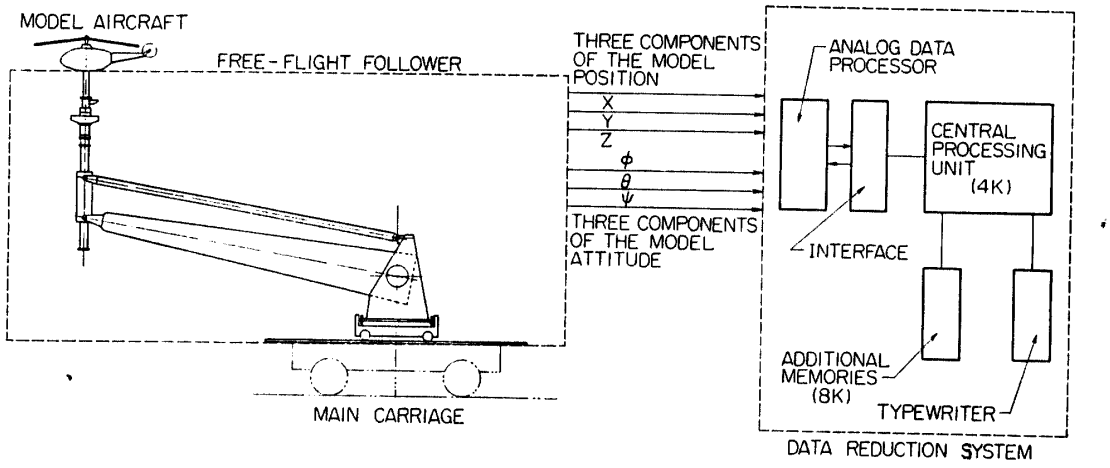

FIG. 1. Block diagram of the total system

SYMBOLS

A: acceleration
AR: aspect ratio
a: speed of sound
C_a: Cauchy number
E: voltage
E: emergy
E: Young's modulus
F: input force
F_r: Froud number
f: reduced frequency
f_t: viscous-friction-torque constant
f_f: viscous-friction-force constant
G: transfer function of the system

G: Modulus of rigidity
G_c: transfer function of the compensating network
G_s: transfer function of uncompensated system
g: gravity acceleration
I: input current
I: moment of inertia
J: moment of inertia of the boom
j: moment of inertia of the movable part of the actuator
K: gain constant
K_A: gain of amplifier
K_F: gain constant of compensated system
K_f: spring force constant
K_M: pressure-force constant
K_P: gain of potentiometer
K_R: pressure torque constant
K_T: gain constant of the total system
K_t: spring-torque constant
K_V: gain constant of the pressure servo valve
l: length of the main boom between two pivotal points
l: density scale factor
M: mass of the follower
M: momentum
M: Mach number
M_p: resonant peak of closed loop
m: mass of the movable parts of the actuator
m: velocity scale factor
m: mass of the model
n: length scale factor
P: power
P: period
p: pressure or stress
Q: moment or torque
R: resistance
R_e: Reynolds number
S: area
s: half of the maximum pursuable range
T: time
T: output torque of the servo system
$T_{1/2}$: time to damp to half amplitude
T_c: time constant of the compensating network
T_{eq}: equivalent time constant
T_r: rise time
T_s: time constant of the servo valve

t: time
t: taper ratio
V: velocity
W: weight or force
X: longitudinal linear displacement of the model aircraft
x: longitudinal slide
x_J: linear displacement of the boom
x_j: linear displacement of the rotary actuator
x_M: linear displacement of the follower
x_m: linear displacement of the oil motor
Y: lateral linear displacement of the model aircraft
y: lateral slide
Z: vertical linear displacement of the model aircraft
z: vertical slide
α: ratio of compensating network
γ: body density
δ: maximum deceleration
Θ: vertical swing angle
θ: pitching angle
λ: Laplace transform parameter
λ: inflow ratio
μ: viscosity
μ: advance ratio
μ: mass ratio
ν: dynamic viscosity
ξ: follower carriage position
ρ: density
σ: rotor solidity
ϕ: rolling angle
Ψ: lateral swing angle
ϕ: yawing angle
Ω: angular momentum
ω: angular velocity
ω_b: brake frequency of open loop
ω_P: resonant frequency of closed loop

SUBSCRIPT

θ, ϕ and ϕ: pitching, rolling and yawing respectively

2. MECHANISM OF FREE-FLIGHT FOLLOWER

A specification for the pursuit performance of the follower may be determined from the previous discussion as given in Table 2. Although the longitudinal motion of the follower on the carriage is limited only on a subtrack installed on the carri-

TABLE 1. Dynamic similarity rule between actual and model aircraft

Items		Symbol	Dimension		Filght Dynamic or Miniature Model	Aerodynamic or Flutter Model		
			LMT System	LFT System		Subsonic	Transonic and Supersonic	Variable Density
Fundamental Physical Quantities	Length	l	L	L	n	n	n	n
	Mass	m	M	FT^2/L	n^3	n^3	n^3	ln^3
	Time	t	T	T	$n^{\frac{1}{2}}$	n/m	n	n/m
	Area	S	L^2	L^2	n^2	n^2	n^2	n^2
	Weight or Force	W	ML/T^2	F	n^3	m^2n^2	n^2	lm^2n^2
	Moment or Torque	Q	ML^2/T^2	FL	n^4	m^2n^3	n^3	lm^2n^3
	Moment or Inertia	I	ML^2	FLT^2	n^5	n^5	n^5	ln^5
	Velocity	V	L/T	L/T	$n^{\frac{1}{2}}$	m	1	m
	Acceleration	A	L/T^2	L/T^2	1	m^2/n	$1/n$	m^2/n
	Angle	θ	1	1	1	1	1	1
	Angular Velocity	ω	$1/T$	$1/T$	$1/n^{\frac{1}{2}}$	m/n	$1/n$	m/n
	Angular Acceleration	$\dot{\omega}$	$1/T^2$	$1/T^2$	$1/n$	m^2/n^2	$1/n^2$	m^2/n^2
	Pressure or Stress	p	M/LT^2	F/L^2	n	m^2	1	lm^2
	Momentum	M	LM/T	FT	$n^{3.5}$	mn^3	n^3	lmn^3
	Angular Momentum	Ω	L^2M/T	LFT	$n^{4.5}$	mn^4	n^4	lmn^4
	Power	P	L^2M/T^3	LF/T	$n^{3.5}$	m^3n^2	n^2	lm^3n^2
	Energy	E	L^2M/T^2	LF	n^4	m^2n^3	n^3	lm^2n^3
Parameters for Body Configuration	Aspect Ratio	AR	1	1	1	1	1	1
	Taper Ratio	t	1	1	1	1	1	1
	Relative Roughness	h/l	1	1	1	1	1	1
	Body Density	γ	M/L^3	FT^2/L^4	1	1	1	1
	Rotor Solidity	σ	1	1	1	1	1	1
Physical Characteristics of Working Fluid	Viscosity	μ	M/TL	FT/L^2	1*	1*	1*	1**
	Dynamic Viscosity	ν	L^2/T	L^2/T	1*	1*	1*	$1/l$**
	Density	ρ	M/L^3	FT^2/L^4	1	1	1	1**
	Speed of Sound	a	L/T	L/T	1*	1*	1*	1**
Aerodynamic Parameters	Mach Number	$M=V/a$	1	1	$n^{\frac{1}{2}}$*	m	1	m**
	Reynolds Number	$\mathrm{Re}=Vl/\nu$	1	1	$n^{1.5}$*	mn*	n*	lmn
	Froude Number	$\mathrm{Fr}=V/\sqrt{gl}$	1	1	1	$m/n^{\frac{1}{2}}$*	$1/n^{\frac{1}{2}}$*	$m/n^{\frac{1}{2}}$*

Configuration	Body Density	γ	M/L^3	FT^2/L^4	1	1	1	1
	Rotor Solidity	σ	1	1	1	1	1	1
Physical Characteristics of Working Fluid	Viscosity	μ	M/TL	FT/L^2	1*	1*	1*	1**
	Dynamic Viscosity	ν	L^2/T	L^2/T	1*	1*	1*	$1/l$**
	Density	ρ	M/L^3	FT^2/L^4	1	1	1	1**
	Speed of Sound	a	L/T	L/T	1*	1*	1*	1**
Aerodynamic Parameters	Mach Number	$M=V/a$	1	1	$n^{\frac{1}{2}}$*	m	1	m**
	Reynolds Number	$\mathrm{Re}=Vl/\nu$	1	1	$n^{1.5}$*	mn*	n*	lmn
	Froude Number	$\mathrm{Fr}=V/\sqrt{gl}$	1	1	1	$m/n^{\frac{1}{2}}$*	$1/n^{\frac{1}{2}}$*	$m/n^{\frac{1}{2}}$*
Flight Dynamic Parameters	Wing or Disc Loading	V/S	M/T^2L	F/L^2	n	m^2	1	lm^2
	Force Coefficients	C_L, C_D	1	1	1	1	1	1
	Moment Coefficients	C_Q, C_M	1	1	1	1	1	1
	Rotor Tip Speed	$R\omega$	L/T	L/T	$n^{\frac{1}{2}}$	m	1	m
	Advance Ratio	μ	1	1	1	1	1	1
	Inflow Ratio	λ	1	1	1	1	1	1
	Cravity Acceleration	g	L/T^2	L/T^2	1	1*	1*	1*
	Acceleration per g or Load Factor	A/g	1	1	1	m^2/n*	$1/n$*	m^2/n*
	Radius of Turn	R	L	L	n	n	n	n
	Period	P	T	T	$n^{\frac{1}{2}}$	n/m	n	n/m
	Time to Damp to Half Amplitude	$T_{\frac{1}{2}}$	T	T	$n^{\frac{1}{2}}$	n/m	n	n/m
	Mass Ratio	$\mu=m/\rho Sl$	1	1	1	1	1	l*
	Time Factor	$\tau=m/\rho SV$	T	T	$n^{\frac{1}{2}}$	n/m	n	n/m
Elastic Parameters	Density Ratio	γ/ρ	1	1	1	1	1	1
	Reduced Frequency	$f=\omega l/V$	1	1	1	1	1	1
	Sectional Moment	$\tilde{I}$	L^4	L^4	n^4	n^4	n^4	n^4
	Bending Rigidity	$E\tilde{I}$	ML^3/T^2	L^2F	n^4*	m^2n^4	n^4	lm^2n^4
	Torsional Rigidity	$G\tilde{J}$	ML^3/T^2	L^2F	n^4*	m^2n^4	n^4	lm^2n^4
	Rigidity Ratio	$G\tilde{J}/E\tilde{I}$	1	1	1	1	1	1
	Cauchy Number	$C_a=E\tilde{I}/\rho V^2l^4$	1	1	l/n*	1	1	1
	Young's Modulus	E	F/LT^2	F/L^2	1*	m^2	1	lm^2
	Modulus of Rigidity	G	F/LT^2	F/L^2	1*	m^2	1	lm^2

n=length of model/length of original plane.
m=velocity of model/velocity of original plane.
l=density of working fluid/density of original fluid for aerodynamic model.
* These quantities contradict the results expected from the dimensional analysis so that the simulation is not satisfied.
** We can change these parameters in model test by selecting adequate working fluids other than air.

TABLE 2. Specification for the pursuit performance

Items	Range	Maximum velocity	Maximum acceleration*	Accuracy for position
Vertical direction	3.5 m	7 m/s	±3 g	±0.3%
Lateral direction	4.0 m	3.5 m/s	±0.5 g	±1.5%
Longitudinal direction	2.4 m	3.5 m/s	±0.5 g	±0.8%
Longitudinal performance of the carriage	185 m	10 m/s	+0.11 g −0.14 g	—

* g is the gravity acceleration.

age, length of which is 2.4 m, the carriage motion of the main track can supplement the performance of the follower. The performance of the carriage is also given in Table 2. There is no positive sensor to detect the carriage position on the main track but the actual position can be obtained either my measuring with a scale along the rail directly or by integration of the carriage velocity which is measured by tachometer dynamos with the accuracy of 0.05 m/s.

To satisfy the above specification, the free-flight follower has been designed as shown in Fig. 2 and Photo 1.

The follower consists of a sliding unit main and sub booms, a follower carriage, actuators, hydraulic sorces, rack rails and other accessories.

The sliding unit can, as shown in Fig. 3, slide vertically in a sheath which is attached to the main and sub booms and holded to keep the unit vertically. Installed on the top of the unit through two sliding boxes is a gimbal system which supports the model via an attachment table so as to let the model have perfect or

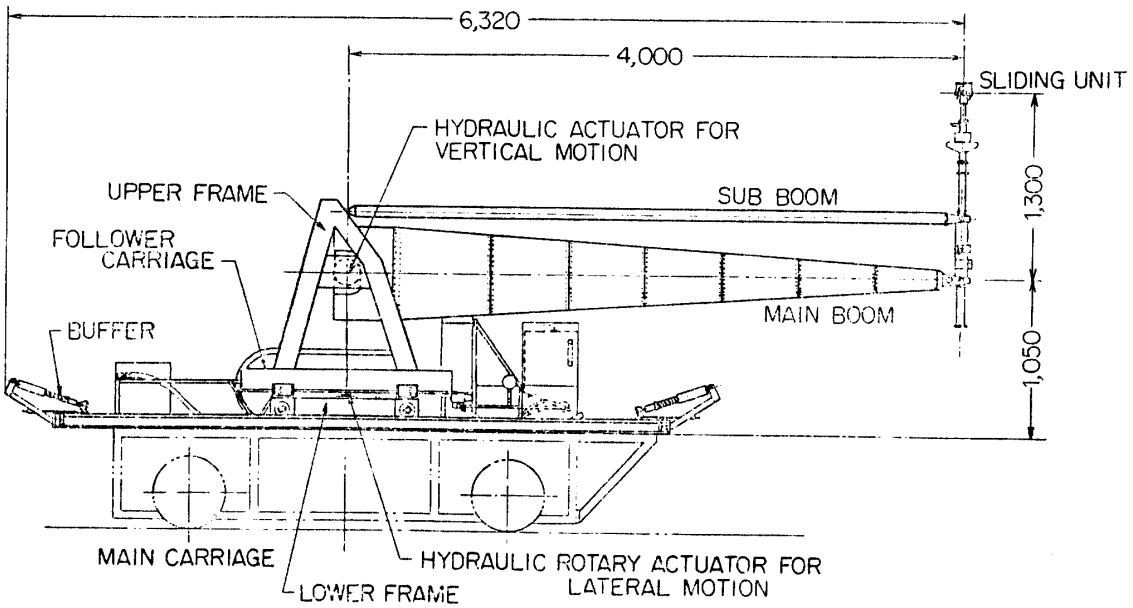

FIG. 2. (a) Side elevation

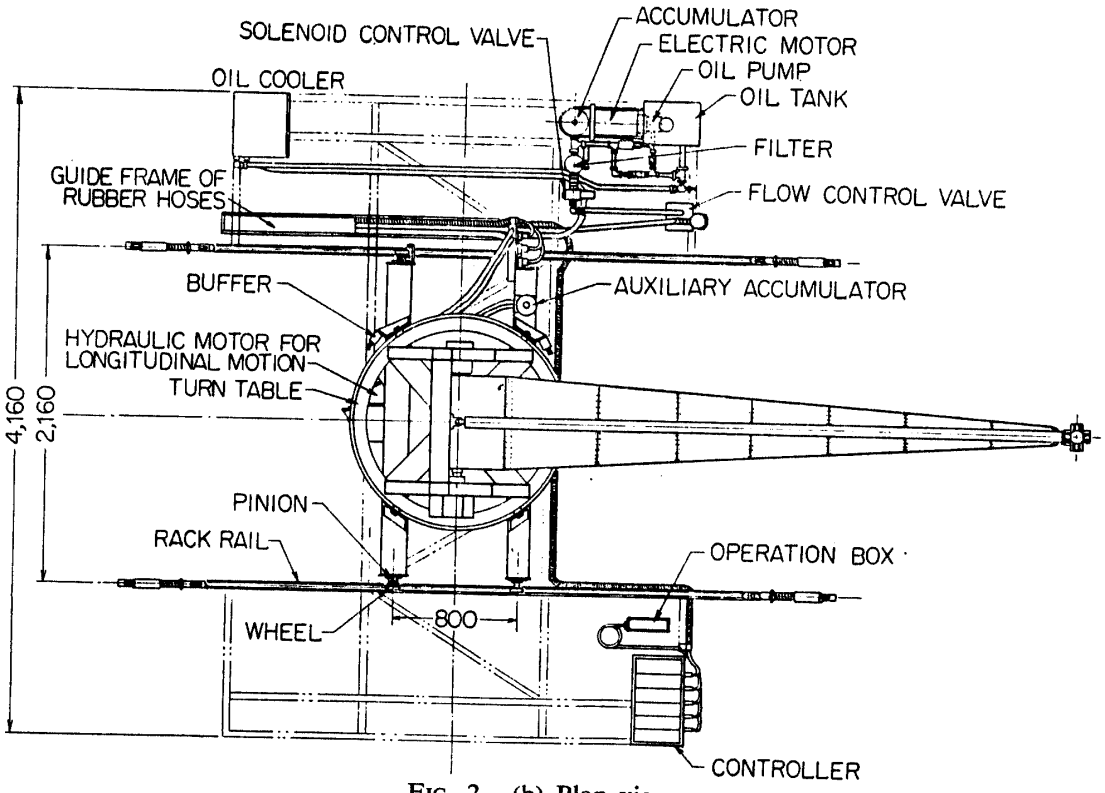

FIG. 2. (b) Plan view

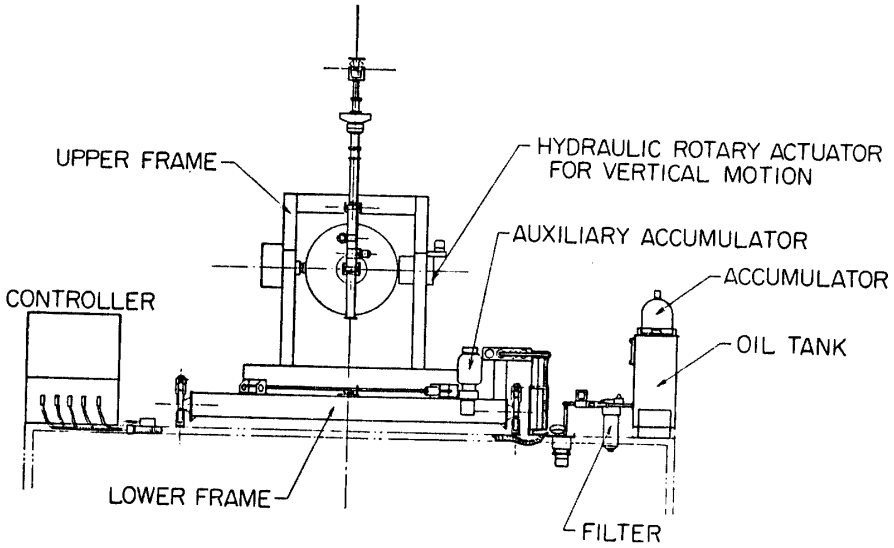

FIG. 2. (c) Frontal elevation

FIG. 2. Mechanism of free-flight follower

partial freedoms for angular motion. The upper part of the gimbal system has two degrees of freedom for pitch and roll and the lower part of the system has a yawing freedom as shown in Fig. 4.

The angular motion of the model can be sensed with three potentiometers each of which is installed on a disc rotating with the model to detect the individual

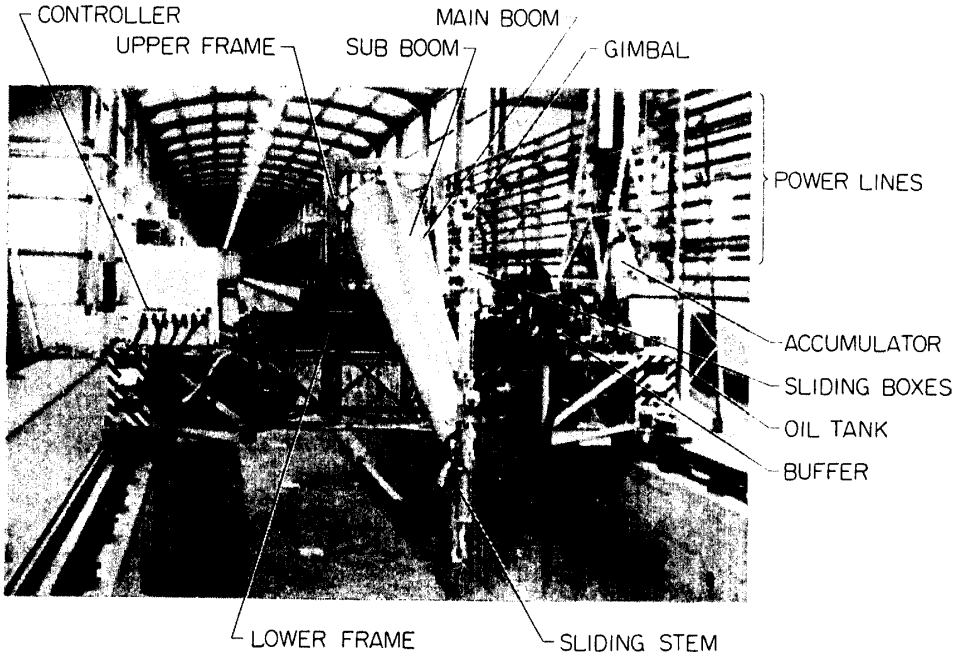

Photo 1. Free-Flight Support System

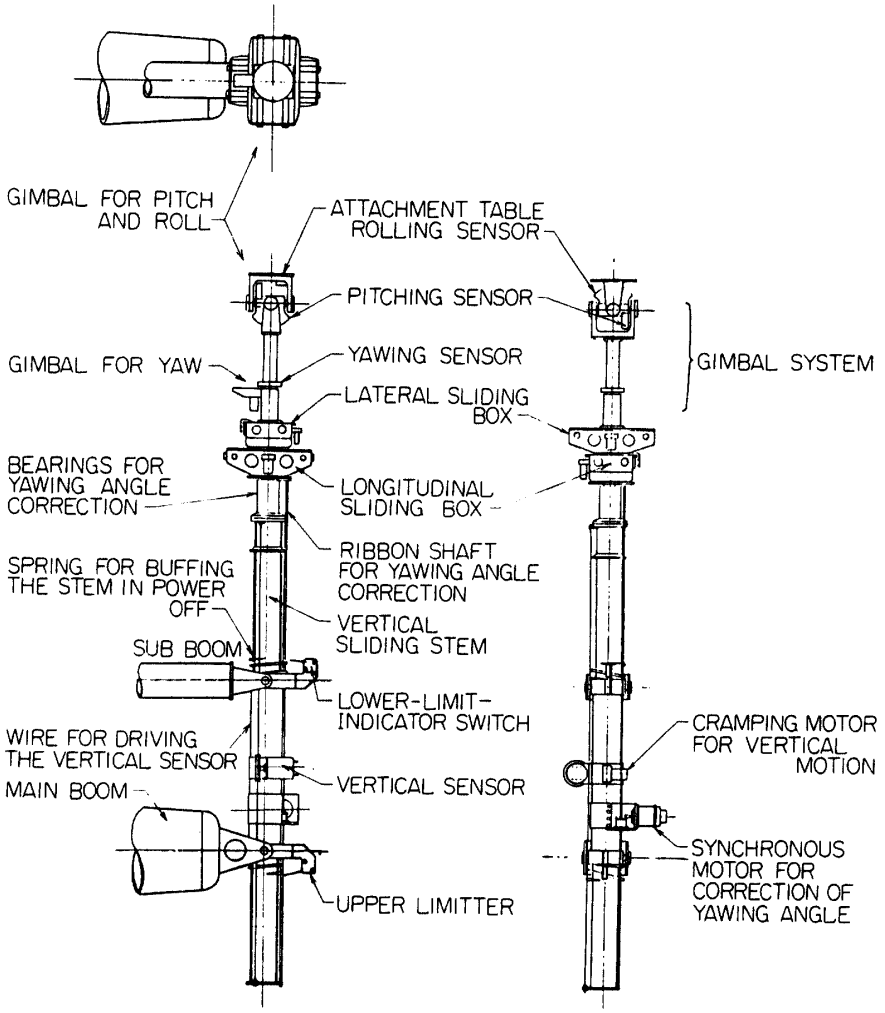

FIG. 3. Sliding unit

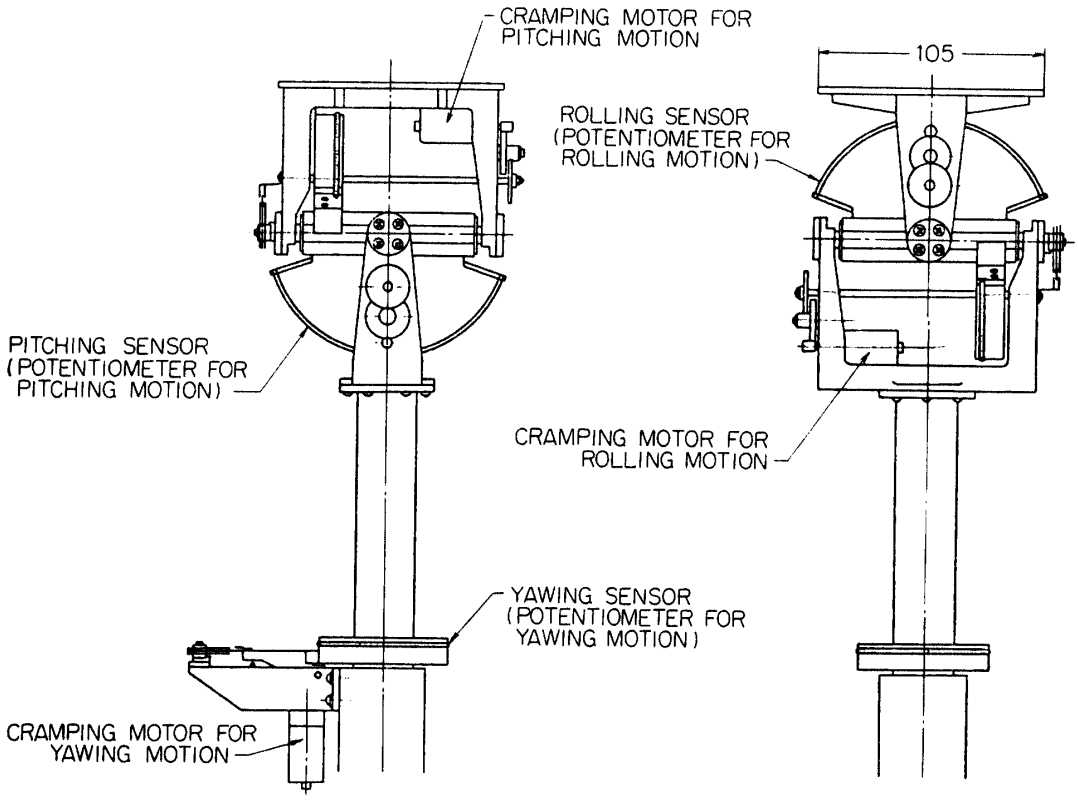

FIG. 4. Gimbal system

TABLE 3. Potentiometers for angular motion

Items	Range (degrees)	Accuracy (degrees)
Pitch	±60°	±0.5°
Roll	±60°	±0.5°
Yaw	±170°	±0.5°

component of the angular motion. The torque of the gimbal due to the friction of the bearings and the potentiometers is less than 0.05 kg/cm for pitch and roll and 0.08 kg/cm for yaw without model. The range which is decided by individual stopper on the gimbal system and the accuracy of the potentiometers are given in Table 3.

The angular motion can be restricted with cramping devices if the motion for undesired direction is wanted to be constrained the cramping of each component is accomplished by hloding the rotational motion of the disc with a braking shoe driven by a servomotor installed on the gimbal system through a train of reduction gears. The cramping torque is about 40 kg/cm. The response time to operate the cramping devices is 0.3 sec. after pushing a button of the control switch in a controller. The excessive inertia moments of the gimbal system which must be added to those of the model are given in Table 4.

As shown in Fig. 5 the lower (longitudinal) and upper (lateral) sliding boxes

TABLE 4. Inertia moments for rotational motion

Items	Moment of inertia ($kg \cdot m \cdot s^2$)
Pitch	5.7×10^{-5}
Roll	8.9×10^{-5}
Yaw	11.4×10^{-5}

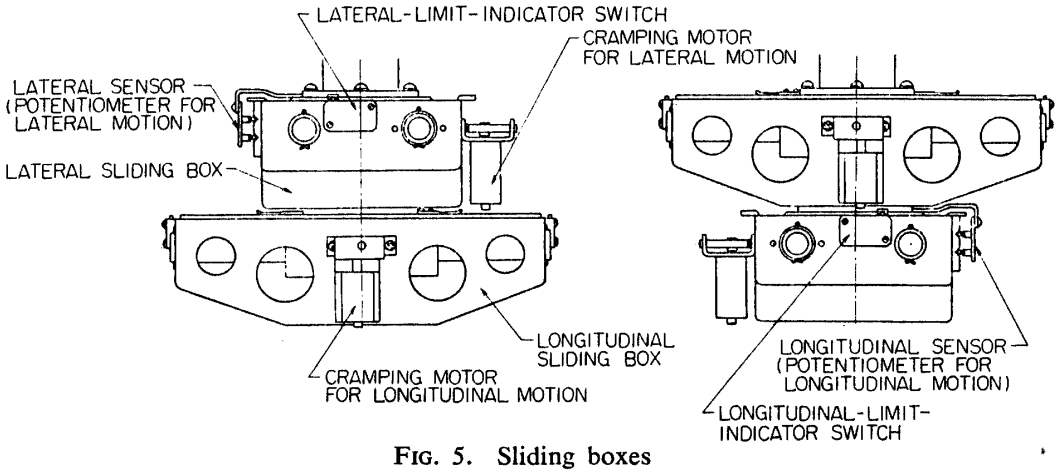

FIG. 5. Sliding boxes

TABLE 5. Range and accuracy of linear motion

Items	Range (m)	Accuracy (%)
Longitudinal	± 0.035	± 1.0
Lateral	± 0.035	± 1.0
Vertical	± 0.250	± 1.0

support the gimbal system so that the model can move freely for longitudinal and lateral directions. To keep the above two degrees of freedom for linear motion of the gimbal system each sliding box has a set of sliding bars for longitudinal and lateral motions so that the gimbal system can move freely in a horizontal plane confined by stoppers along the bars through the bearings, the friction of which is less than 0.05 kg without model.

The linear motion along each direction is detected with individual potentiometer installed outside of the box and can be constrained if necessary. The ranges and accuracies of the linear motion in the sliding box are given in Table 5.

The excessive masses for lateral and longitudinal motion of the model are given in Table 6.

The cramping of each component of linear motion is performed by the actuation of individual knock pin which is driven by each servo motor installed on the box through a train of reduction gears. The response time of the cramping is 0.1 sec.

TABLE 6. Additional mass for linear motion

Items	Mass (kg·s²/m)
Longitudinal	0.27
Lateral	0.16
Vertical	0.51

after pushing a button of the control switch in the controller.

Each linear motion on the sliding box is detected by a couple of sliding potentiometers, one of which is used for recording of the data and the other is used as a feedback signal to make the follower take necessary action by which the model can always stay at the center of the bar.

It must be interesting to say that the sliding boxes are supported on the sliding unit to keep always the longitudinal direction of the longitudinal sliding box being parallel and the lateral direction of the lateral sliding box being normal to the track. For this purpose the unit is provided with a compensation mechanism consisted of a pair of synchronous motors one of which is located on the rotational center of the main boom as a sensor of the rotational angle of the boom and the other is installed on the sheath, as shown in Fig. 3, as an actuator to rotate the stem to compensate the rotational angle caused by the boom rotation in a horizontal plane. The actuator of the synchronous motor can drive a strip about its vertical axis. Installed on the upper end of the strip is a pinion which is meshed with and drives a gear fixed to the sliding unit. The strip can slide vertically between two rollers with the sliding unit so that the compensation can be obtained during the vertical motion of the model. It seems to be more convenient and accurate to provide the above compensation mechanism for the data reduction of the linear motion of the model than to make it by analogous way with electric resolvers.

The lower part of the sliding unit under the sliding boxes can slide inside of the sheath. The sliding motion of the unit in vertical direction is sustained by two sets of radial bearing which are installed on opposite ends of the sheath respectively and hold two protuberances machined along the front and back sides of the sliding unit so that the unit can not turn about the vertical axis as shown in Fig. 3. The friction force of the vertical sliding motion is less than 0.05 kg.

The vertical motion is detected by a potentiometer installed on the sheath. The drum of the potentiometer is coiled and driven by a string, terminals of which are fixed to the opposite ends of the sliding part of the sliding unit. The allowable range of the vertical motion of the unit and the accuracy of the potentiometers are also given in Table 5.

Two outputs of the potentiometer for vertical position are used as an input to the recorder and a feedback signal respectively to make the follower take necessary action by which the center of the sliding part of the unit can always be located in middle or neutral position of the sheath during a test.

The sliding motion of the unit can also be cramped by a knock pin driven by

a servomotor. Once the knock pin has been retracted and the sliding motion has been initiated the cramping can not be operated from remote position. As the protection of the system, two coiled springs are put on the upper and lower sections of the sliding part to bump the shock which might be expected after one run of the test.

The sliding unit must have proper rigidity to persue and detect the model motion with necessary accuracy. The bending and torsional rigidities are given in Table 7 while the total weight of the unit is 5 kg.

The main and sub booms support the sliding unit with the sheath as a pantograph mechanism so that the center lines of both booms, the sheath and the follower carriage make a parallelogram as shown in Fig. 2a. The both booms are pivoted on the follower carriage and can be swinged up and down in parallel.

The main boom is driven by a hydraulic rotary actuator installed on a upper frame of the follower carriage within a range of $\pm 22°$ which corresponds to a range of ± 1.5 m for the vertical motion of the sheath. Since the shear forces and moments due to the weight and inertia forces of the system are loaded only on the main boom the construction of the main boom must be as light as possible and yet be strong enough to bear the above loads. The boom may, therefore, be a shell structure formed to a cone type as shown in Fig. 2. An aluminum plate, thickness of which is 0.5 mm, is rolled on and riveted to vertical ring frames to make a cone. The weight of the main boom is 9 kg. The bending and torsional rigidities of the boom are given in Table 8.

The upper frame is constructed with welded steel tubes having rectangular cross section so that the weight is low and yet the rigidity is high.

The rotary actuator is operated by a feedback signal of the vertical position error of the sliding unit so that the follower can keep the unit to stay always in neutral position. The sub boom is a single tube, one end of which is pivoted on the upper part of the sheath and the other end is pivoted on the upper frame so that the tube serves only to keep the vertical attitude of the sheath.

The lateral linear motion of the model can be obtained by swinging the boom horizontally with the rotation of the upper frame. The upper frame of the follower

TABLE 7. Rigidity of the sliding unit

Items	Rigidities
Bending	2.7 mm/kg
Torsion	9.2×10^{-3} rad/kg·m

TABLE 8. Rigidity of the main boom

Items	Rigidities
Bending	0·22 mm/kg
Torsion	3.2×10^{-4} rad/kg·m

carriage which supports the booms is constructed on a turn table and hence can rotate about a vertical axis passing through two pivotal points of the main and sub booms on the follower carriage. The turn table is cramped with four pairs of the guide wheels and driven by a hydraulic rotary actuator installed on a lower frame to rotate the upper frame with itself.

The actuator of the lateral motion is operated by a feedback signal of the position error which is detected by the lateral potentiometer in the upper sliding box so that the model can always be sustained in laterally neutral position of the sliding box. The range of the lateral motion is $\pm 30°$, which is equivalent to the linear motion of ± 2.0 m at the model position.

The construction of the lower frame is wholly same as that of the upper frame.

To pursue the linear motion of the model in longitudinal direction the lower frame of the follower carriage set on four wheels can move on a track consisted of two rails, length of which is 4.0 m. A hydrauli motor is installed on the lower frame and drives two pinions, each of which is couppled with a rack rail attached to the individual rail of the track. Thus the longitudinal motion of the follower carriage can be attained by the actuation of the hydraulic motor stimulated from a feedback signal of the position error of the longitudinal potentiometer in the lower sliding box so that the model can always be sustained in longitudinally neutral position of the sliding box. To prevent the lateral and directional motions

TABLE 9. Mass, moments of inertia and driving powers related to each component of the follower carriage.

Items	Mass ($kg \cdot s^2/m$)	Moments of inertia ($kg \cdot m \cdot s^2$)	Driving Power ($kg \cdot m/s$)
Vertical	4.8	9.7	125
Lateral	4.8	9.7	10.4
Longitudinal	29.2	0.0111	500

of the follower carriage on the track there are two pairs of guide wheels on the one side of the lower frame, which cramp the both sides of one rail. The other four wheels are provided on the lowe frame to hold the carriage so as to never lift off.

There are four buffers installed on the opposite ends of both rails to absorve the shock which might be expected to the extreme flight condition. The range of the longitudinal motion is, therefore, limited to 2.8 m between front and rear buffers. The mass, moments of inertia and the driving powers related to each component of the follower carriage are given in Table 9.

Installed on the upper and lower frames there are two potentiometers to detect the rotational motions in vertical and horizontal planes respectively. To detect the longitudinal motion of the follower carriage with respect to the main carriage a potentiometer is installed on the lower frame. The outputs of these potentiometers are utilized to measure the model position as will be described in later.

3. Measurements of Attitude and Position

To measure the model attitude and position in space total nine potentiometers have been installed on the follower as shown in Fig. 6. The sensed quantities and output forms are listed in Table 10.

The attitude angle of the model can be obtained from the potentiometers of No. 1 through No. 3 directly as Eulerian angles of body coordinate system. As shown in Fig. 7, the outputs of the potentiometers which are obtained from the supplied voltages per unit length of the potentiometers, E_1, E_2 and E_3, will be

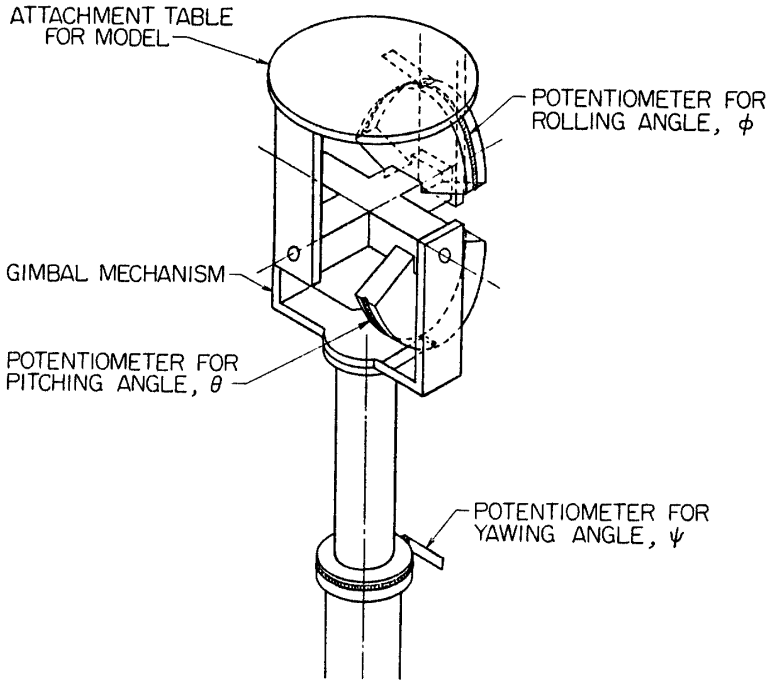

Fig. 6. (a) Attitude Sensors

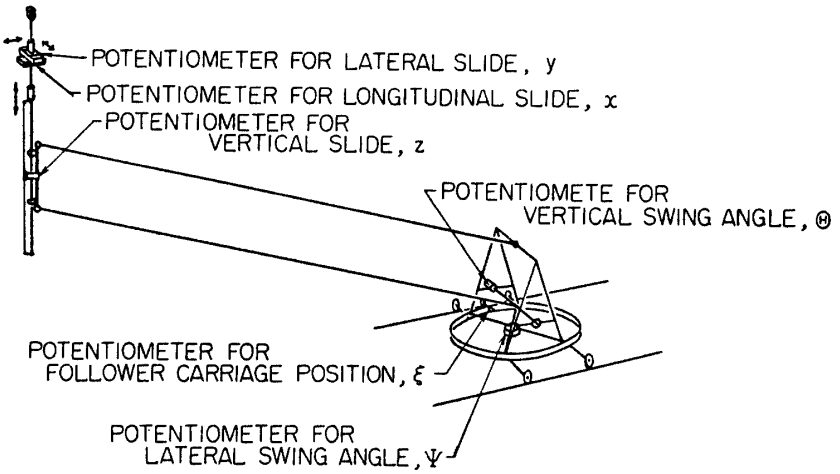

Fig. 6. (b) Position sensors

Fig. 6. Arrangements of sensors

TABLE 10. Potentiometers

No.	Sensed quantities	Symbols	Output forms	Locations
1	Rolling angle	ϕ	Angular type	Gymbal system
2	Pitching angle	θ	Angular type	
3	Yawing angle	ψ	Angular type	
4	Longitudinal slide	x	Linear type	Sliding box
5	Lateral slide	y	Linear type	
6	Vertical slide	z	Linear type	Sheath
7	Vertical swing angle	Θ	$\cos\Theta$ and $\sin\Theta$	Upper frame
8	Lateral swing angle	Ψ	$\cos\Psi$ and $\sin\Psi$	Lower frame
9	Follower carriage position	ξ	Linear type	Lower frame

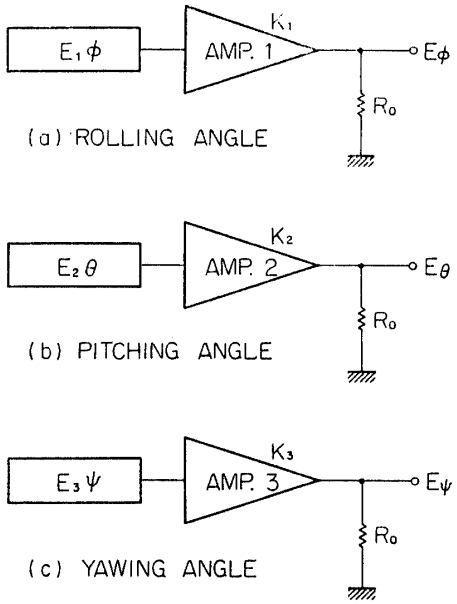

FIG. 7. Circuits for Eularian angles

amplified in amplifiers, 1, 2 and 3 which are inpedance tranceducers connected to recorders. The output voltages, E_ϕ, E_θ and E_ψ, are given by

$$\left.\begin{aligned} E_\phi &= K_1 E_1 \phi \\ E_\theta &= K_2 E_2 \theta \\ E_\psi &= K_3 E_3 \psi \end{aligned}\right\} \qquad (1)$$

where K_1, K_2 and K_3 are gains of the amplifiers for rolling, pitching and yawing components respectively.

The range and accuracy of the measured angles for attitude are given in

TABLE 11. Range and accuracy of attitude angle measurements

Items	Range		Accuracy (%)
	Angles (degrees)	Voltages (Volt)	
Rolling angle	±60°	±0.600	±0.8
Pitching angle	±60°	±0.600	±0.8
Yawing angle	±170°	±1.700	±0.3

Table 11.

The position or linear displacement of the model in space is given by the following formulae:

$$\left.\begin{aligned} &\text{Longitudinal component: } X \\ &\qquad X = x + \xi - l(1 - \cos\Theta\cos\Psi) \\ &\text{Lateral component: } Y \\ &\qquad Y = y + l\cos\Theta\sin\Psi \\ &\text{Vertical component: } Z \\ &\qquad Z = z + l\sin\Theta \end{aligned}\right\} \qquad (2)$$

wherein l is length of the main boom between two pivotal points.

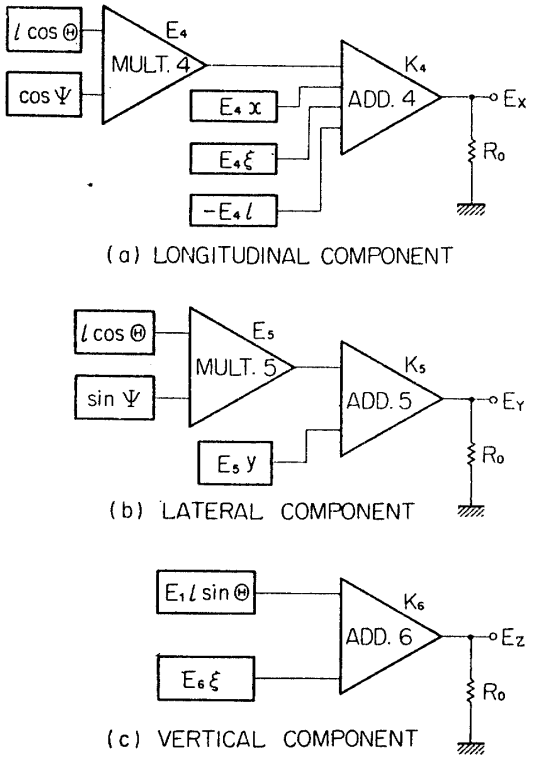

FIG. 8. Circuits for linear displacement

As shown in Fig. 8, the outputs of the potentiometers which are obtained from the supplied voltages per unit length of the potentiometers, $E_4 \sim E_6$, will be multiplied or added and amplified in multipliers [4, 5], or adders [4–6], in which amplifiers are impedance transducers connected to recorders. The output voltages, E_X, E_Y and E_Z are given by

$$\left.\begin{aligned} E_X &= K_4 E_4\{x+\xi-l(1-\cos\Theta\cos\Psi)\} \\ E_Y &= K_5 E_5\{Y+l\cos\Theta\sin\Psi\} \\ E_Z &= K_6 E_6\{z+l\sin\Theta\} \end{aligned}\right\} \qquad (3)$$

The range and accuracy of the measured length and trigonometric functions of boom-swing angles for position are given in Table 12.

TABLE 12. Range and accuracy of position measurements

Items		Range		Accuracy (%)
		Length (mm)	Voltage (V)	
Longitudinal slide, x		±35	±0.007	±1.0
Lateral slide, y		±35	±0.007	±1.0
Vertical slide, z		±250	±0.050	±1.0
Follower carriage position, ξ		±1,350	±1.350	±0.2
Trigonometric functions,	$\cos\Theta$	±22	1.054 (at 0°)	±0.3
	$\cos\Psi$	±30	2.828 (at 0°)	±0.3
	$\sin\Theta$	±22	2.828 (at 22°)	±0.3
	$\sin\Psi$	±30	1.054 (at 30°)	±0.3
Longitudinal motion, X		±1,200	±0.240	±0.8
Lateral motion, Y		±2,000	±0.400	±1.5
Vertical motion, Z		±1,500	±0.300	±0.3

4. SERVO SYSTEM

As described before, the follower must pursue the linear motion of the model during the dynamic test. To accomplish the above follower operation a servo system is assembled. The system is consisted of hydraulic servo mechanisms having three driving units, or vertical, lateral and longitudinal driving units, electronic units and a hydraulic power source to make up the feedback systems for the follower operation. The hydraulic servo mechanism must be useful as an actuator having good response and high power but light weight characteristics.

In driving units, two rotary actuators [1, 2], are installed on the upper frame of

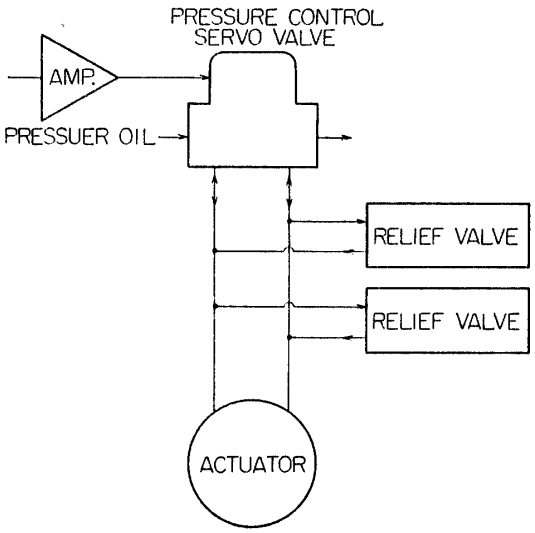

FIG. 9. Block dyagram of actuator operation

the follower to swing the boom vertically and laterally and one hydraulic motor is installed on the lower frame of the follower for longitudinal motion.

The above actuators or motors can be driven with a pressurized working oil through a servo valve as shown in Fig. 9. The working oil is pressurized by an oil pump driven by an electric motor which is regulated by a pressure switch, 1, to

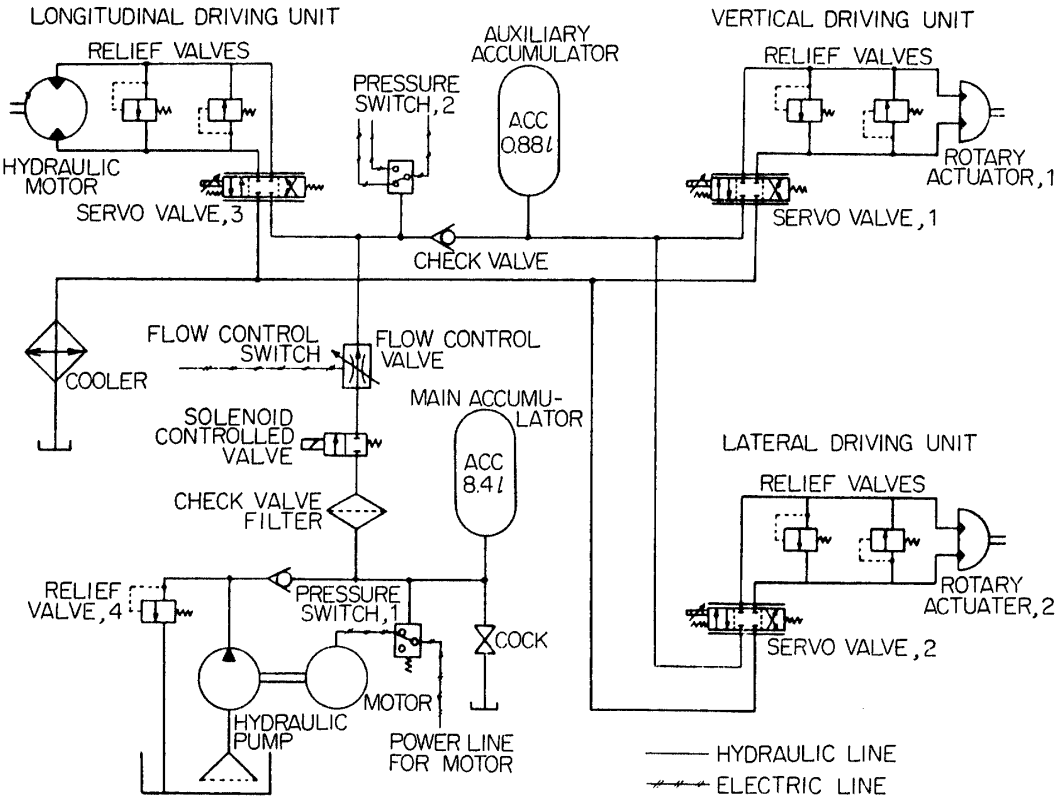

FIG. 10. Hydraulic circuit diagram

TABLE 13. Specifications of the pump and accumulators

Items	Numbers
The maximum allowable pressure	210 kg/cm²
Volume of the main accumulator	8.4 *l*
Volume of the anxiliary accumulator	0.88 *l*
Trapped nitrogen gas pressure in the main accumulator	120 kg/cm²
Effective exhaust flow	1.37 *l*
The maximum working pressure	175 kg/cm²
The minimum working pressure	140 kg/cm²
Exhaust flow rate of hydraulic pump	8.5 *l*/min
Output of driving motor for hydraulic pump	3.7 KW

keep a specified range of pressure given in Table 13, and is always stored in a main accumulator so that the powers and, therefore, the volumes of the pump and the motor can be reduced. The specifications of the pump and the accumulator are given in Table 13. The hydraulic circuit diagram is shown in Fig. 10.

To vivify the power source a solenoid controled valve must be operated. This can be done only when a flow control valve is off condition, which is provided between the solenoid controled valve and the servo valves and serves to protect the system from an abnormal operation. In an emergency such as electric power off or oil loss in operation, an auxiliary accumulator must be effective to bring the boom in neutral position by operation of an emergency circuit. The pressure of the trapped gas in the auxiliary accumulator is less than that of the main accumulator so that in normal operation the oil is alway stored in the both accumulators. If the pressure of the main accumulator drops, a pressure switch [2], provided between the auxiliary accumulator and the flow control valve senses the pressure change and operates the emergency circuit. Provided between the main and auxiliary accumulators is a check valve which prevents the reverse flow of the oil to the main accumulator. As a matter of course, for abnormal increase of the hydraulic pressure seven relief valves are provided in individual driving unit and the pressure source.

The vertical or lateral (linear) motion at the tip of the boom, length of which is l, may be schematically expressed by an equivalent dynamic system as shown in Fig. 11. The equations of motion of the equivalent system for the linear displacements of the rotary actuator and the actuated boom, x_j and x_J respectively, can be given by

$$\left.\begin{aligned} j\ddot{x}_j+f_t(\dot{x}_j-\dot{x}_J)+K_t(x_j-x_J)&=Tl \\ J\ddot{x}_J-f_t(\dot{x}_j-\dot{x}_J)-K_t(x_j-x_J)&=0 \end{aligned}\right\} \qquad (4)$$

where T is an input torque, j and J are moments of inertia of the movable parts of the actuator and the actuated boom respectively, and f_t and K_t are viscouse friction- and spring- torque constants respectively. These parameters of the system are given in Table 14.

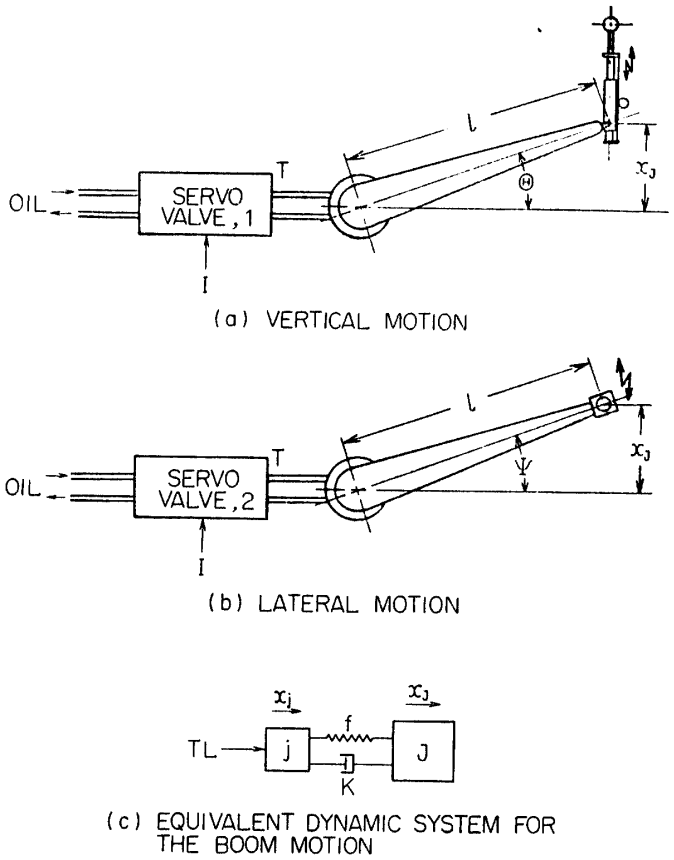

FIG. 11. Equivalent dynamic system for the vertical and lateral boom motion

Then, the transfer function of the output, x_J, due to the input torque, T, will be given by

$$x_J/T=\frac{l(f_t\lambda+K_t)}{\lambda^2\{jJ\lambda^2+f_t(j+J)\lambda+K_t(j+J)\}} \tag{5}$$

where λ is a Laplace-transform parameter. Usually the moment of inertia of the actuator can be neglected comparing with the mass of the actuated boom so that the above equation can be approximated as

$$x_J/T\fallingdotseq l/J\lambda^2 \tag{6}$$

A transfer function of the output torque, T, of the servo valve with respect to an input current, I, can be given by

$$T/I=K_VK_R/(T_S\lambda+1) \tag{7}$$

where K_V is a gain constant of the pressure-servo valve, K_R is a pressure-torque constant and T_S is a time constant of the servo valve.

The block diagram of the present servo system in vertical or lateral motion can, thus, be shown as Fig. 12a.

TABLE 14. Parameters of the equivalent systems

	Items	Symbols and dimension	Vertical motion	Lateral motion	Longitudinal motion
Follower mechanics	Moment of inertia of the actuator	j(kg·m·s²)	6×10^{-5}	2×10^{-5}	—
	Moment of inertia of the boom	J(kg·m·s²)	10×10^{1}	2×10^{1}	—
	Vescous-friction-torque constant	f_t(kg·m·s)	6×10^{1}	1.5×10^{1}	—
	Spring-torque constant	K_t(kg·m)	8×10^{3}	3×10^{3}	—
	Mass of the actuator	m(kg·s²/m)	10^{-2}	—	—
	Mass of the follower	M(kg·s²/m)	2.9×10^{1}	—	—
	Viscous-friction-force coefficient	f_f(kg·s/m)	2.5×10^{1}	—	—
	Spring-force constant	K_f(kg·m)	5×10^{3}	—	—
Pressure-servo valve	Gain of servo valve	k_V(kg/cm²·mA)	2.1×10^{1}	2.1×10^{1}	2.1×10^{1}
	Pressure-force constant	K_R(cm³)	10^{2}	3.6×10^{1}	—
		K_V(cm²)	—	—	1.55
	Time constant	T_S(s)	5×10^{-3}	5×10^{-3}	5×10^{-3}
Amplifier	Gain of potentiometer	K_P(V/cm)	10^{-2}	10^{-2}	10^{-2}
	Gain of amplifier	K_A(mA/V)	4.2×10^{2}	1.9×10^{3}	2.6×10^{3}
Compensating network	Time constant	T_c(s)	1×10^{-1}	1×10^{-1}	1×10^{-1}
	Ratio	α(1)	10^{1}	10^{1}	10^{1}

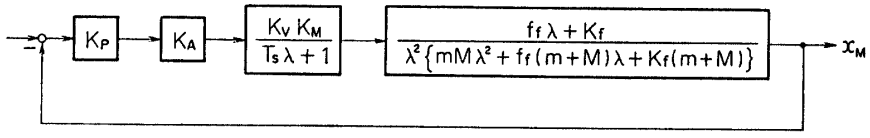

(a) UNCOMPENSATED SYSTEM

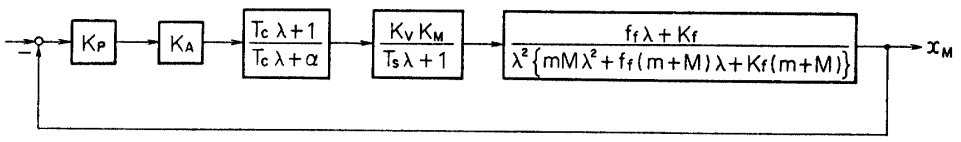

(b) COMPENSATED SYSTEM

FIG. 12. Block diagrams of the servo system for vertical and lateral motions

An over all transfer function in open loop of the servo system will become

$$\left.\begin{aligned} G_s(\lambda) &= \frac{lK_V K_R K_P K_A (f_t\lambda + K_t)}{\lambda^2\{jJ\lambda^2 + f_t(j+J)\lambda + K_t(j+J)\}(T_s\lambda+1)} \\ &\doteqdot \frac{lK_V K_R K_P K_A/J}{\lambda^2(T_s\lambda+1)} \end{aligned}\right\} \quad (8)$$

The following compensating network may be desirable to improve the response characteristics of the system:

$$G_c(\lambda) = (T_c\lambda+1)/(T_c\lambda+1) \quad (9)$$

where adequate system parameters are selected as shown in Table 14.

The total transfer function of the compensated servo system shown in Fig. 12b is, then, given by

$$\left.\begin{aligned} G(\lambda) &= G_s(\lambda)G_c(\lambda) \\ &\doteqdot \frac{K_t(T_c\lambda+1)}{\lambda^2(T_s\lambda+1)\{(T_c/\alpha)\lambda+1\}} \end{aligned}\right\} \quad (10)$$

where

$$K_T = lK_V K_R K_P K_A/J\alpha \quad (11)$$

The longitudinal motion of the follower can, also, be expressed by an equivalent dynamic system as shown in Fig. 13. The following analysis will be obtained in similar way to the preceding discussion. The equations of motion of the equivalent system for the linear displacements of the oil motor and the actuated follower, x_m and x_M respectively, caused by an input force, F, can be given by

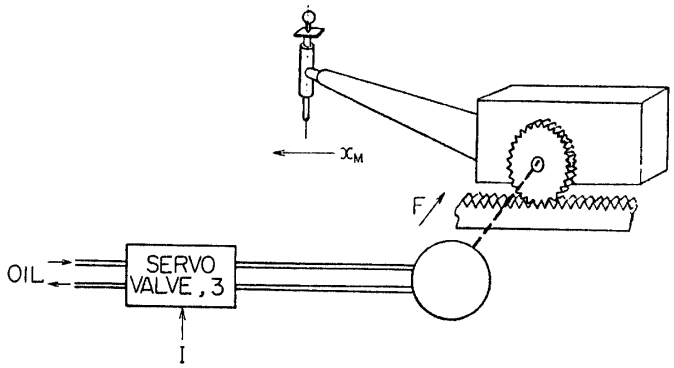

(a) LONGITUDINAL MOTION

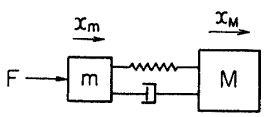

(b) EQUIVALENT DYNAMIC SYSTEM FOR THE CARRIAGE MOTION

FIG. 13. Equivalent dynamic system for the longitudinal follower motion

$$\left.\begin{aligned} m\ddot{x}_m + f_f(\dot{x}_m - \dot{x}_M) + K_f(x_m - x_M) = F \\ M\ddot{x}_M - f_f(\dot{x}_m - \dot{x}_M) - K_f(x_m - x_M) = 0 \end{aligned}\right\} \tag{12}$$

where m and M are masses of the movable parts of the actuator and the actuated follower respectively, and f_f and K_f are viscous friction- and spring-force constants respectively. These parameters of the system are also given in Table 14.

The equations (12) yield the transfer function of the output, x_M, due to the input force, F, as follows:

$$\left.\begin{aligned} x_M/F &= \frac{f_f\lambda + K_f}{\lambda^2\{mM\lambda^2 + f_f(m+M)\lambda + K_f(m+M)\}} \\ &\doteqdot 1/M\lambda^2 \end{aligned}\right\} \tag{13}$$

A transfer function of the output force, F, of the servo valve with respect to an input current, I, can similarly be obtained as

$$F/I = K_V K_M/(T_s\lambda + 1) \tag{14}$$

where K_M is a pressure-force constant.

The block diagram of the present servo system in longitudinal motion can, thus, be shown as Fig. 14a and the open-loop-transfer function of the system is given by

$$\left.\begin{aligned} G_s(\lambda) &= \frac{K_V K_M K_P K_A(f_f\lambda + K_f)}{\lambda^2\{mM\lambda^2 + f_f(m+M)\lambda + K_f(m+M)\}(T_s\lambda + 1)} \\ &\doteqdot \frac{K_V K_M K_P K_A/M}{\lambda^2(T_s\lambda + 1)} \end{aligned}\right\} \tag{15}$$

By using the same kind of compensating network as that given by the equation (10), the total transfer function of the compensated system shown in Fig. 14b becomes

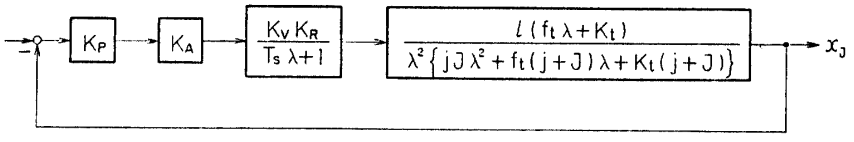

(a) UNCOMPENSATED SYSTEM

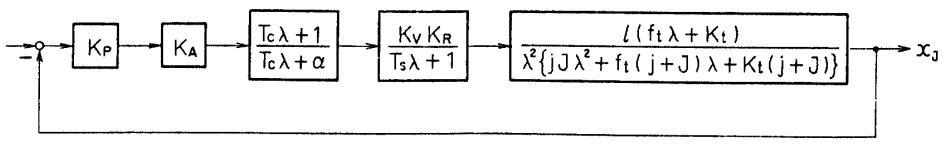

(b) COMPENSATED SYSTEM

FIG. 14. Block diagrams of the servo system for longitudinal motion

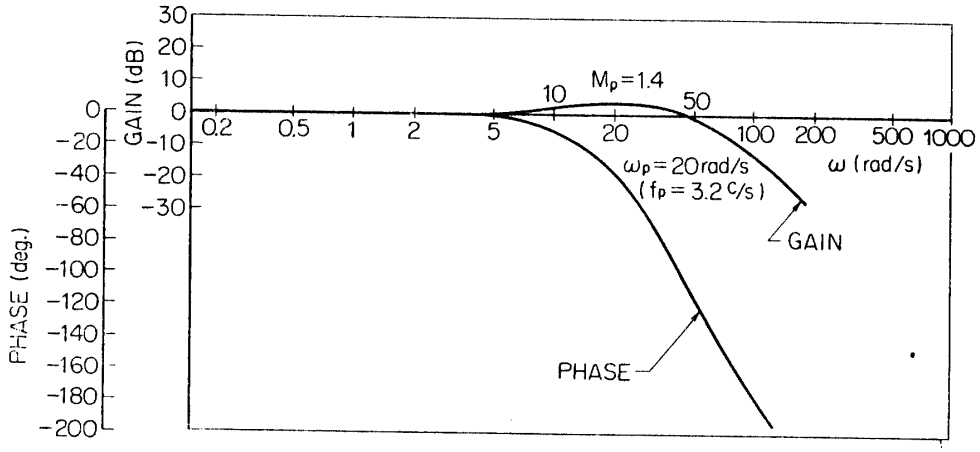

FIG. 15. (a) Vertical motion

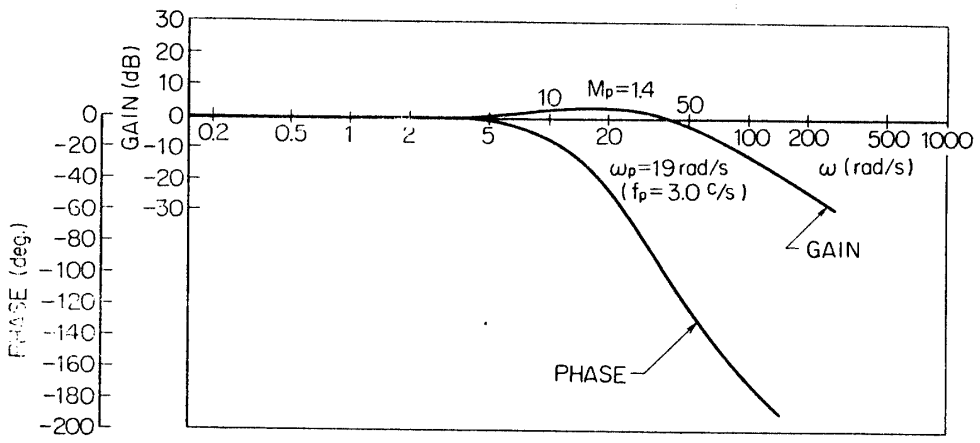

FIG. 15. (b) Lateral motion

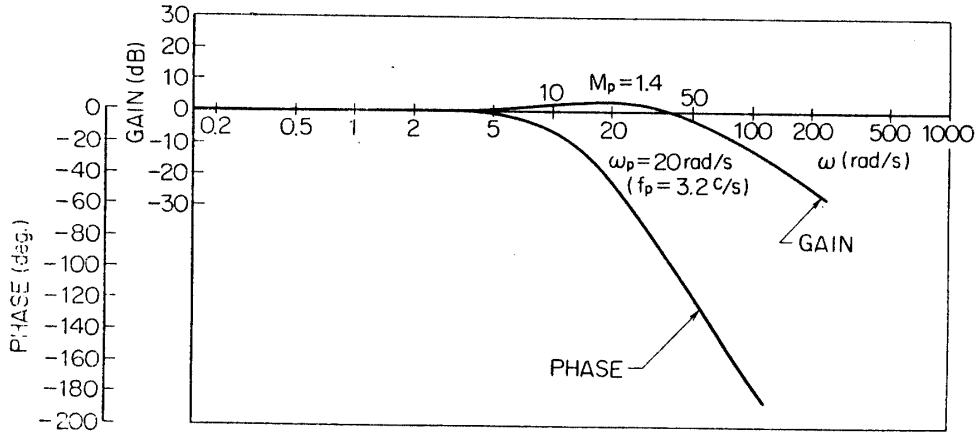

FIG. 15. (c) Longitudinal motion

FIG. 15. Bode diagram of the compensated system

$$\left.\begin{aligned} G(\lambda) &= G_s(\lambda)G_c(\lambda) \\ &\doteqdot \frac{K_F(T_c\lambda+1)}{\lambda^2(T_s\lambda+1)\{(T_c/\alpha)\lambda+1\}} \end{aligned}\right\} \tag{16}$$

where

$$K_F = K_V K_M K_P K_A / M\alpha \tag{17}$$

TABLE 15. Dynamic characteristics of the servo system

Items	Symbols and dimension	Vertical motion	Lateral motion	Longitudinal motion
Break frequency of open loop	ω_b(rad/s)	30	27	25
Resonant peak of closed loop	M_p(1)	1.4	1.4	1.4
Resonant frequency of closed loop	ω_p(rad/s)	20	20	20
Equivalent time constant	T_{eq}(s)	0.043	0.037	0.033
Rise time	T_r(s)	0.065	0.065	0.068

Each component of the compensated total system in closed loop is characterized by Bode diagram as shown in Fig. 15 and Table 15. Although not shown in figure, the rise times obtained from actual responses of the boom motion for given step inputs show good agreement with the calculated values given in Table 15.

5. Operation of Free-Flight Follower

The free-flight follower can be operated by either manual or automatic proce-

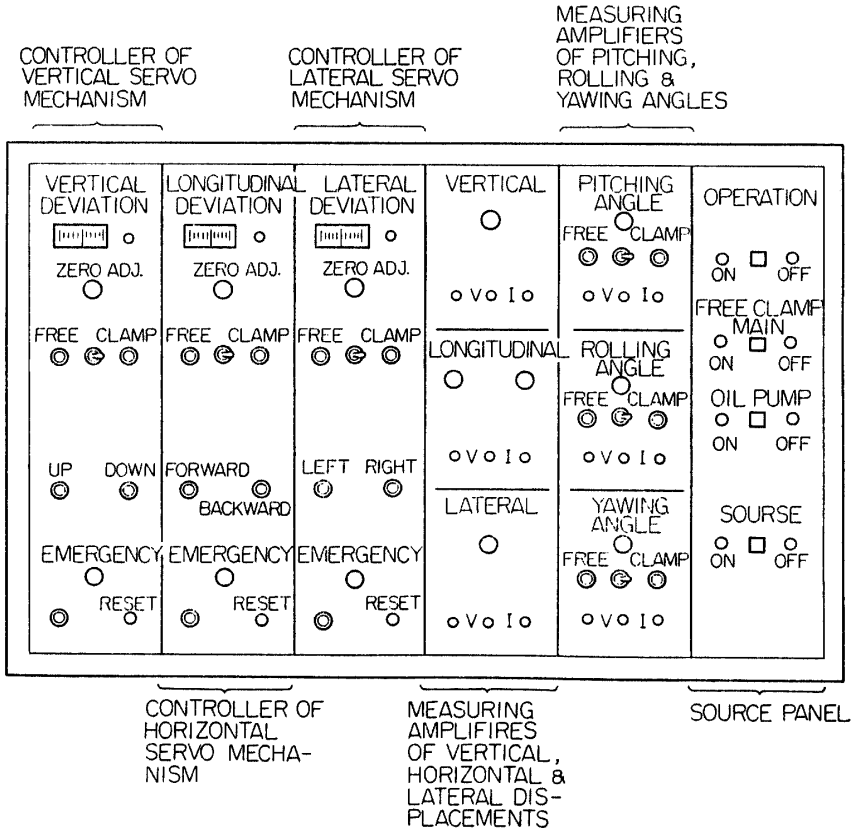

FIG. 16. Controller

dures. Fig. 16 and 17 show a controller and an operation box of the free-flight support system respectively. Fig. 18 gives an electric circuit diagram of the system.

In manual operation an operator seating on the main carriage can control the attitude of the main boom and longitudinal position of the follower by turning any of three knobs on an operation box (Fig. 16). The speed of the follower and the boom swing velocity can be adjusted by the rotational speed of the knob.

In automatic pursuit operation any motion of a model aircraft installed on the top of the sliding unit can automatically be followed by the boom and the follower motions without disturbing the model motion.

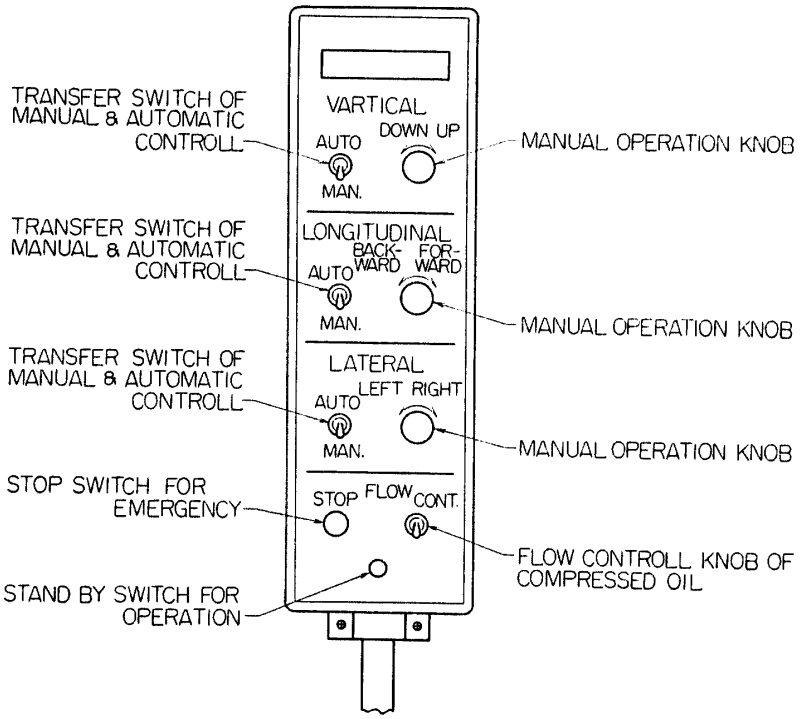

FIG. 17. Operation box

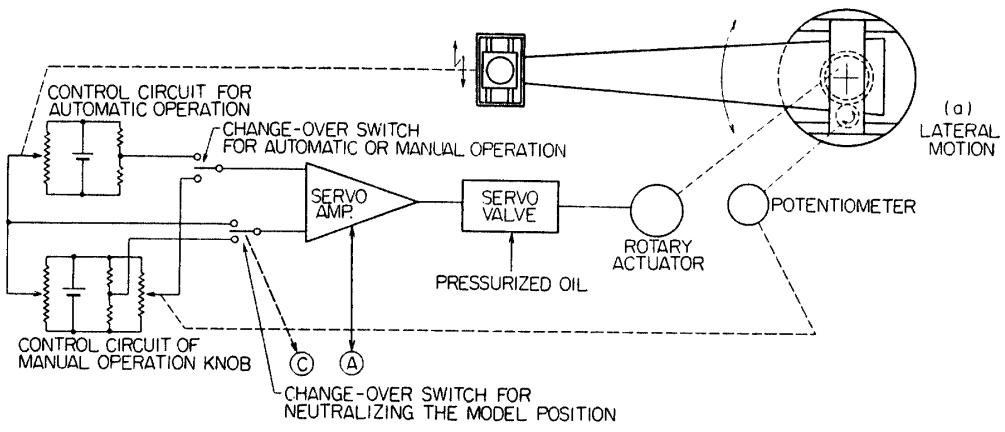

(a)

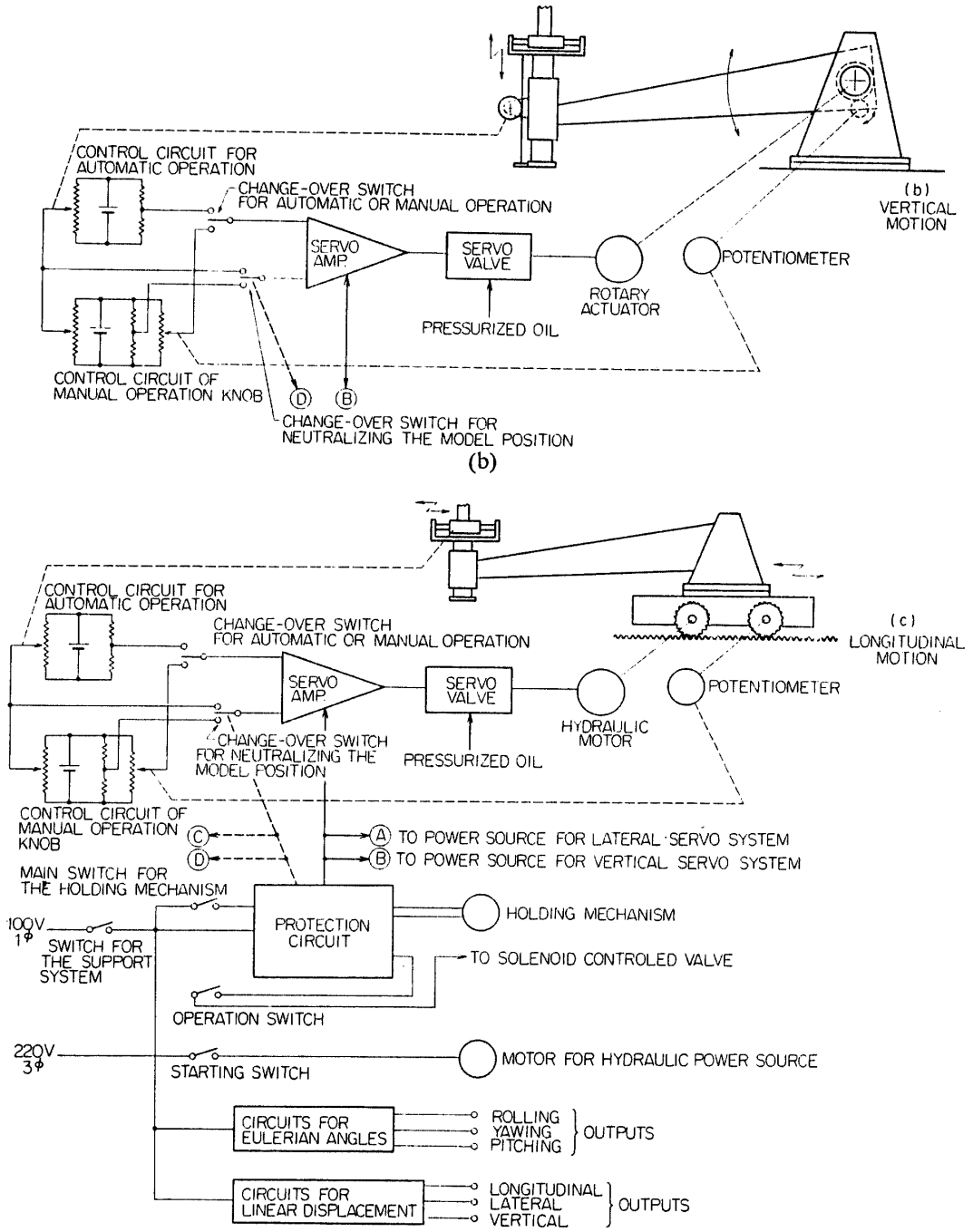

FIG. 18. (c) Electric circuit diagram

6. PROTECTION SYSTEMS

To protect the follower in extreme condition or emergency there are three kinds of protection systems such as mechanical, electric and hydraulic protection systems.

A solid stopper is installed on the upper frame to limit the maximum upward vertical motion. The lower limit of the vertical motion is restricted by a vane stopper of the rotary actuator. For the lateral motion of the boom a pair of buffers

is provided on the lower frame to restrict the extreme swinging motion of the upper frame in left or right direction. For the longitudinal motion of the follower additional buffers are also provided at the opposite ends of the rails. The buffer is a kind of hydraulic type stopper as shown in Fig. 19 and is designed to operate for the speed less than 1 m/s without any damage.

Electric protection system are represented by a protection circuit as shown in Fig. 20. Six micro switches[*1*]~[*6*], are installed on the opposite ends of the sliding bars and sliding stems as limit switches and if the flight model behaves abnormally beyond the maximum pursuable speed of the follower any one of switches is pushed by the model just before touching the mechanical terminal end. Then, a buzzer which is prepared in the controller alarms an abnormal operation. Furthermore, if the follower carriage approaches to the end of the rail a micro switch[7], which is installed on the follower carriage is pushed by one of protuberances fixed on the opposite ends of the rail just before the buffer. Similarly,

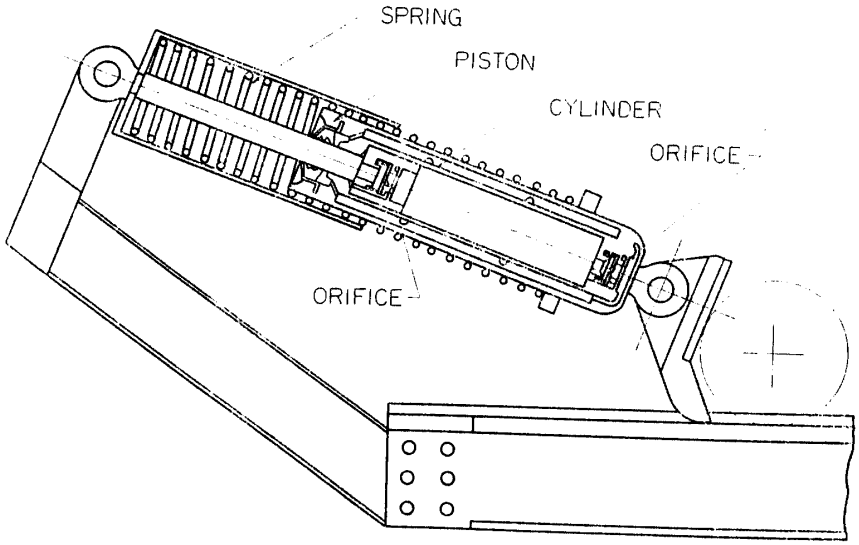

FIG. 19. Buffer

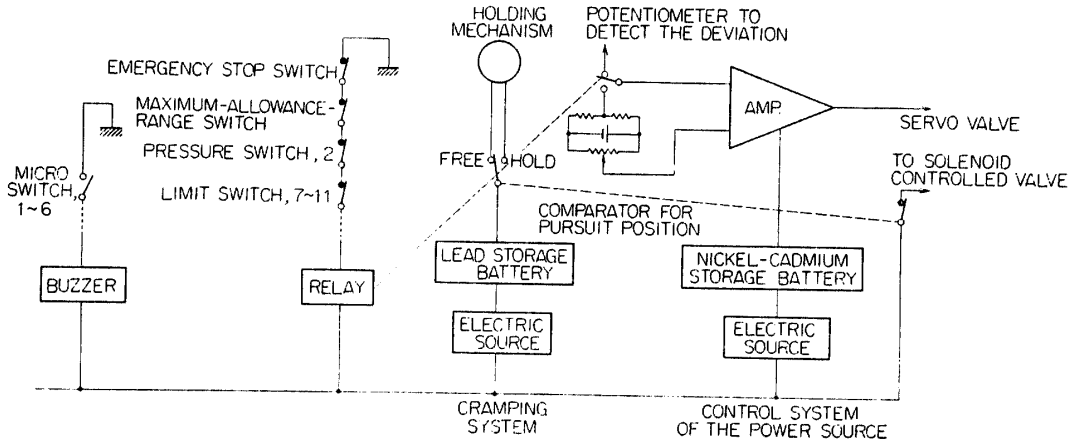

FIG. 20. Protection circuit

two pairs of limit switches [8]~[11], are prepared on the upper and lower frames for limitting the vertical and lateral swing motion of the main boom respectively. The switches will be pushed at the limit end of the swing motion. By the above any one of switching actions a relay for emergency operation is activated and automatic cramping devices, each of which can hold the rotational motion of the model with friction created by a cramping motor installed on the gimbal, are operated as has been stated and the solenoid controlled valve is shut off to restrain the model motion. Simultaneously, a protection device for hydraulic pressure drop will be operated as will be described in later.

The model is, thus, cramped on the support system the boom of which reverts to the neutral position and, then, descends to the lowest position with the sliding stem by gravity. As aforesaid, a spring installed on the sheath of the sliding unit will buff the motion of the sliding stem at the final stage of the descending motion. The longitudinal motion of the follower carriage on the rails is braked by pumping action of the hydraulic motor, the acceleration of which is regulated by two relief valves connecting the input and output ports of the hydraulic motor.

Allowable range of the boom motion must be limited to protect the model and the support system from the destruction due to the collision with the walls and floors of the buildings and the pit. This range must also be holded in a power failure of the hydraulic or electric system. An auxiliary accumulator, the settling pressure of which is less than that of the main accumulator, is provided to hold the model and to return the boom to the neutral position in an emergency, such as power off, by detecting the pressure drop of the main accumulator with the pressure switch [2], and activating the relay for emergency operation, as also aforesaid.

For an electricity failure, a nickel-cadmium storage battery and a lead storage battery are provided in the control system of the power source and in the cramping systems respectively and supplement the system operation following to the hydraulic power failure.

When the pursuit speed of the follower in any direction is over a specified value which is, as will be described in later, determined to stop the boom or follower motion within the allowable range with the maximum deceleration the protection circuit is operated.

This protection system in the longitudinal pursuing motion will be explained as an example by referring to Fig. 21. The speed of the follower carriage with respect to the main varriage, V, can be obtained from an AC generator directly connected to the hydraulic motor as a DC voltage, E_V, by rectifying the AC output

$$E_V = KV \tag{18}$$

where K is a proportional constant.

A root function generator, which is a potentiometer interlocked to the rack rail, generates a voltage, as shown in Fig. 21b, corresponding to the longitudinal follower position as follows:

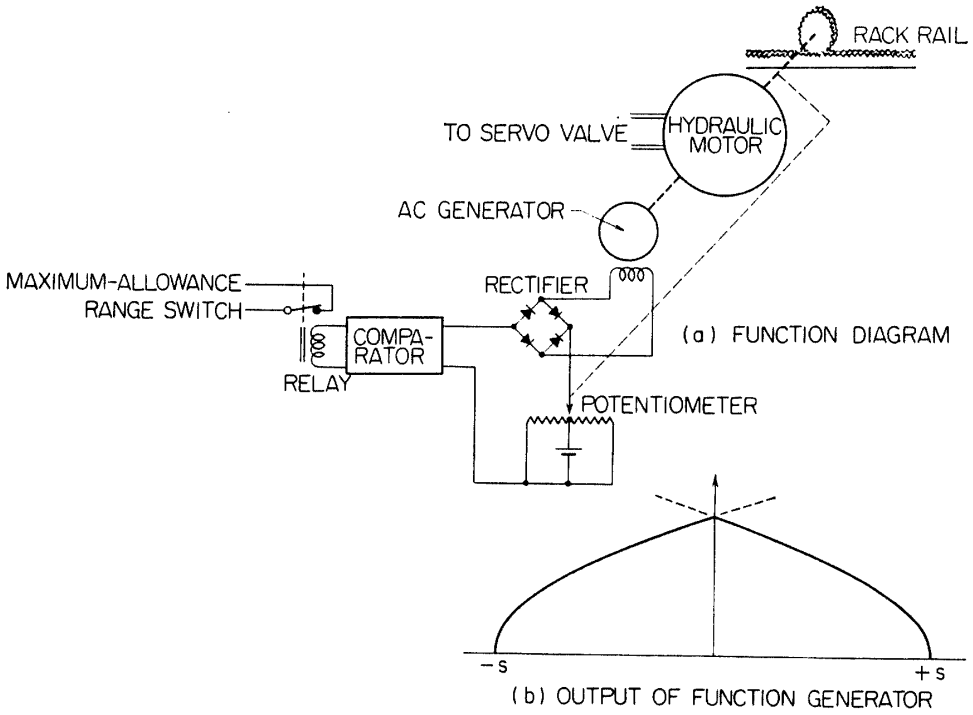

FIG. 21. Function diagram of the maximum-sllowance-range switch

$$\left.\begin{aligned} E_x &= K\sqrt{2\delta(s+x)} \qquad \text{for } -S<X<0 \\ &= K\sqrt{2\delta(s-x)} \qquad \text{for } S>X>0 \end{aligned}\right\} \tag{19}$$

where δ is a maximum deceleration and s is a half of the maximum pursuable range. When the voltage proportional to the follower speed is over the above specified value or

$$\Delta E = E_V - E_X > 0 \tag{20}$$

a comparator gives an output to operate a maximum-allowance-range switch which has same function as those of the limit switches, and stops finally the pursuit operation.

7. DATA REDUCTION SYSTEM

A data reduction system mainly consists of a HITAC-10 mini-computer system and comprises an analog data processor, a central processing unit (C.P.U.) and its extended memory unit, a data typewriter, H-9331-41FD, and a high-speed-perforated-tape reader, H-8226-2. (See Photo. 2)

The analog data processor is a general name of an assembly consisted of a pre-amplifier, a data recorder, TEAC-R250, and an analog-digital converter, H-1613-2.

Provided for low-speed- and high- speed- data inputs and outputs of the C.P.U. is an input-output interface by which the C.P.U. can be connected to a plurality of low-speed- data input and output equipments and simultaneously be operated

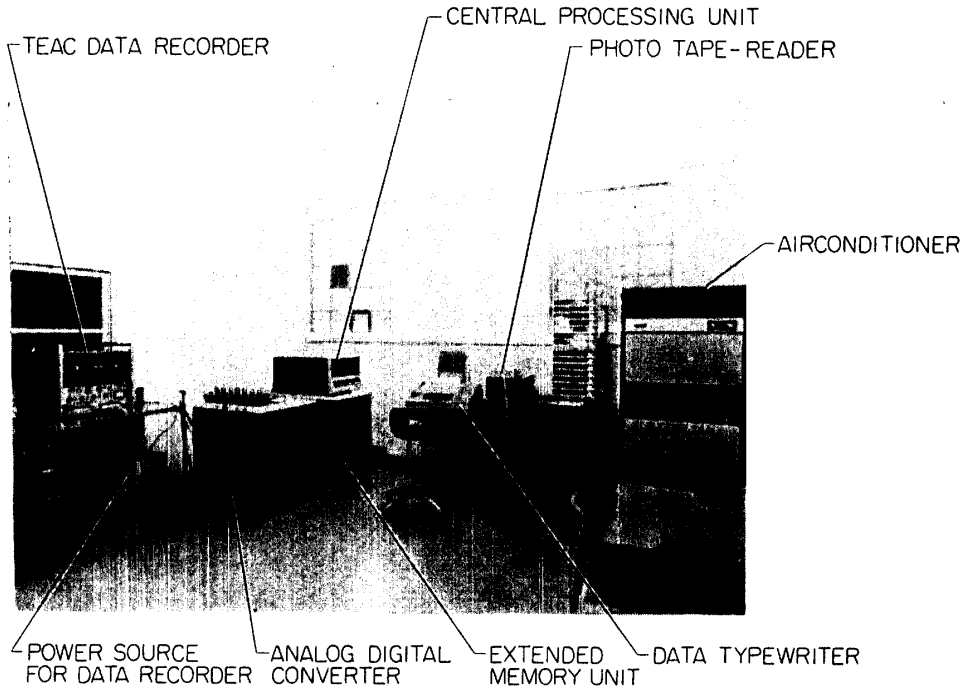

Photo 2. Data Reduction System

for multichannel inputs and outputs. The C.P.U. can also be connected to a high-speed-data input and output equipment through the input-output interface but when the C.P.U. is connected to a plurality of high-speed-data input and output equipments the time shared processing may be performed by connecting a data channel multiplexer, H-P1610-24.

The C.P.U. is, as shown in Fig. 22, composed of a basic processing unit having 4K words core memories, H-1610, a basic extension control, H-P1610-2, a basic extended memory module (4K words), H-P1610-21, an extented arithmetic element, H-P1610-11, an automatic restart control, H-P1610-23, a timer control,

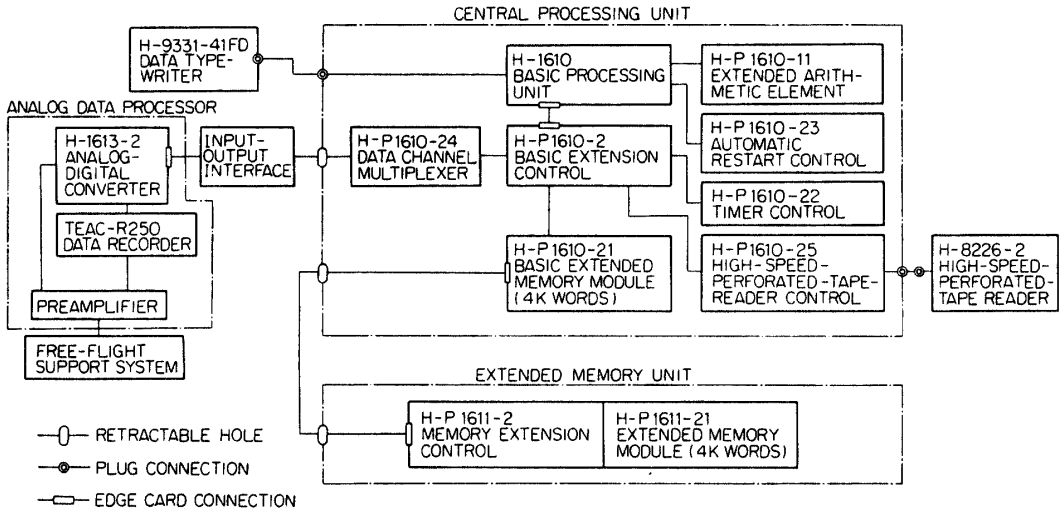

FIG. 22. Block diagram of data reduction system

H-P1610-22, a high-speed-perforated-tape-reader control, H-P1610-25, and the said data channel multiplexer. As the additional memory equipment the extended memory unit contains a memory extension control, H-P1611-2, and an extended memory module, H-P1611-21, (4K words) in an independent rack.

The analog data processor can receive analog and digital inputs and release digital outputs after processing by a specified instruction.

The functions of other equipments will be self-evident from their nominations.

Sensed data by the free-flight support system are amplified by the preamplifier and are transfered either directly or through the data recorder to the analog-digital converter which is connected to the input-output interface.

Data processed in the C.P.U. under a given instruction are typed out by the data typewriter or recorded on a tape at the data typewriter.

8. Conclusion

A support system for free-flight of model aircraft simulated to V/STOL plane or helicopter has been constructed for the study of aero and/or flight dynamics. The data obtained from the support system can be analyzed in a data reduction system by a specified instruction. The above support system and the data reduction system have been prepared for the supplementary equipment of the running test facility reported in Ref. 1. The total cost of the above two systems was about $120,000.

Department of Aerodynamics
Institute of Space and Aeronautical Science
University of Tokyo
December 15, 1971

References

[1] Azuma, Akira et al.: A New Running Test Facility for the Study of Flight Dynamics. Institute of Space and Aeronautical Science, University of Tokyo, Report No. 437, March 1969.

[2] Pankhurst, R. C.: Dimensional Analysis and Scale Factors. The Institute of Physics and The Physical Society by Chapman and Hall Limited, London Reinhold Publishing Corporation, New York, 1964.

[3] Abbott, Ira H.: Theory of Wing Sections. Dover Publications, Inc. New York, 1949.

[4] Perkins, Courtland D. and Hage, Robert E.: Airplane Performance Stability and Control. John Wiley & Sons, Inc. New York, London, Sydney, 1949.

[5] Jacobs, Eastman N. and Sherman, Albert: Airfoil Section Characteristics as Affected by Variations of the Reynolds Number. NACA Rep. 586, 1937.

[6] Bisplinghoff, Raymond L., Ashley, Holt and Halfman, Robert L.: Aeroelasticity. Addison-Wesley Publishing Company, Inc. Reading, Mass., 1955, pp. 695–748.

Appendix

Similarity Laws in Flight Dynamic, Aerodynamic and Aeroelastic Problems

In the field of flight dynamics, aerodynamics and aeroelasticity, the experimental investigation with scaled models is sometimes very helpful for the development of useful theory and estimation of related quantities on an objective aircraft. In order to simulate the actual behaviour of the aircraft with a properly scaled model the dimensional analysis [2] must carefully be applied.

In the present problems length, either mass or force and time are selected as "primary quantities" to be measured directly in units of their own kinds and are treated as independent of one another. The other physical quantities are derived from the primary quantities according to some rule of combination, which are then called "secondary quantities." By selecting either mass or force a system is known as LMT or LFT system. We have discarded temperature as a primary quantity since we do not want to treat the hypersonic aerodynamics which must be combined with thermodynamics. A speed of sound of working fluid is, then, considered to be unchanged in model test.

To obtaine the dimensional properties to be designed into the model, three independent scale factors are introduced here such as:

$$\text{Length scale factor, } n=\frac{\text{length of model}}{\text{length of original aircraft}}$$

$$\text{Velocity scale factor, } m=\frac{\text{velocity of model}}{\text{velocity of original aircraft}}$$

$$\text{Density scale factor, } l=\frac{\text{density of working fluid}}{\text{density of air}}$$

Some combinations of the scale factors for various parameters in the flight dynamic and aerodynamic or flutter models comparing with their dimensions are shown in Table 1.

The length scale factor, n, descides the model dimension and is, therefore, limited for practical and economic reasons less than 1.

The velocity scale factor, m, is usually determined from wind tunnel speed used in model test or model speed in free flight test. In subsonic problem, such as stall, the Reynolds number is an essential factor to be simulated. Usually, it is not easy to simulate the Reynolds number because both the model scale and the test speed are small comparring with the original. Then, the test should be performed as much as higher Reynolds number than, at least, a "critical Reynolds number [*3, 4*] specifically for a rounded body. From the test beyond the critical we can estimate the related aerodynamic quantities to a certain degree by extraporation [*4, 5*].

For transonic and supersonic tests the velocity scale should be m=1 because

the Mach number becomes an important parameter to satisfy a condition that the values of dimensionless variables determined from the π theorem [2] must be the same for both the original problem and its model.

In the aeroelastic or flutter tests, the vibration frequency is an important factor. The velocity scale can be selected to fit the vibration frequency either to the best frequency range of the measuring equipment which is available or to the visible frequency range by naked human eye or by high speed camera for complete understanding of the flutter mode since the time scale is decided from the ratio of length scale to velocity scale, or n/m.

In flight dynamic model, however, the independent relationship between n and m must be abandoned. As far as the model test is performing on the earth the gravity acceleration, g, can not be scaled so that acceleration per g or load factor which is an essential parameter for flight dynamic simulation of the model will exclusively be governed by the acceleration only. The acceleration scale in the present system is given by m^2/n the flight dynamic simulation requires a relation of $m^2/n=1$ or $m=\sqrt{n}$. This is very important design limitation for the flight dynamic model unless otherwise the test is performed on planets other than earth.

In aerodynamic or flutter simulation model the nondimensional aerodynamic and flutter parameters should be simulated to the original problem i.e. the parameters should be the same values for both the original and the model as much as possible. It is, therefore, desirable to use the air with variable density or some other gas such as Freon as a working fluid. By proper combination of the density scale factor, l, with the m and n the physical characteristics of working fluid and, specifically, the aerodynamic parameters can widely satisfy the expected values in the test*. Since the speed of sound in the air is dependent on its temperature we can regulate the Mach number by changing the temperature of the air. If we can adopt some gas other than the air more variety in the aerodynamic parameters may be expected.

In the flight dynamic model it is almost impossible to keep the simulation for the all elastic parameters if the model structure is constructed with same materials as those of the original aircraft. This tendency can be improved in the aerodynamic or flutter model by changing the materials specified from the square of velocity scale factor, m^2. This will impose a certain restriction for the selection of the model materials. If we want more free selection of the model materials the velocity scale must be limited as far as Cauchy number is in our consideration.**

As a summary the following conclusions have been obtained from Table 1:

(1) All scale factors of the fundamental physical quantities and parameters for body configuration do not contradict with the results of dimensional analysis for

---

* Instead of specifying the temperature and pressure of the working fluid the density and speed of sound of the fluids are given as controlable parameters.

** To allow free selection of the model materials an elasticity scale factor, p, might be introduced instead of the density scale factor.[6] In such simulation model, however, the Cauchy number will be given by p/m^2. To make this number to be nondimensional or 1, p must be $p=m^2$ which is just same as the aerodynamic model.

any model.

(2) In the items of the physical characteristics of working fluids and the aerodynamic parameters, the scale factors can, usually, not satisfy the simulation i.e. the results are different from those obtained by dimensional analysis. Such quantities are shown with an asterisc in the Table 1. This tendency can be improved by introducing the variable density air or some other working fluid other than air.

(3) Almost all scale factors of the flight dynamics are satisfied for the simulation. The acceleration per g or load factor is the most important one of exceptions. This simulation can be attained only in the case of $m^2=n$.

(4) The elastic parameters can be simulated by careful selection of the materials and the proper mass distribution.